

## The Outer Ionosphere at Mid- and Low Latitudes

*I. S. Kutiev*

### Introduction

Satellite data came first within our reach in 1969, with the beginning of joint investigations with the working team of Galperin from the Space Research Institute in Moscow on the joint usage of ground-based data and of data obtained from the COSMOS-261 and COSMOS-348 satellites. In 1969 broad-scale research work was started in cooperation with the working team of Prof. Gringaus from the Space Research Institute in Moscow, in the field of the processing and geophysical interpretation of the measurements of ion density, made by INTERCOSMOS-2 satellite. These were the first for Bulgaria methodological investigations on the processing and interpretation of the volt-ampere characteristics of the spheric ion traps. That resulted in the establishment of reliable methods for the separation of oxygen and carbon ions which have found a broad application in further experiments. The first Bulgarian instrument, jointly developed by our Institute and the working team of Gringaus, was a combination of spheric ion traps and the Langmuir cylindrical probe, applied aboard INTERCOSMOS-8 in 1972. On the grounds of the data obtained from these two satellites in the Central Laboratory for Space Research there were conducted a number of studies on the structure of the equatorial outer ionosphere, on the longitude peculiarities in the distribution of ion density under the conditions of a geomagnetic field, on the structure and time variations of the midlatitude trough, etc. Probe instruments for sounding the ionospheric plasma flew later on aboard the INTERCOSMOS-12, 14 and 18 as ingredient of scientific payload with different purposes. With the help of INTERCOSMOS-12 there was studied the behaviour of the midlatitude trough at an altitude of 700 km, with special attention being paid to the behaviour of the  $O^+$  and  $H^+$  ions. The INTERCOSMOS-14 was aimed at studying the waves occurring in the outer ionosphere where passive measurements were made only of the variations of the ion density by means of a spherical ion trap. Spherical ion traps and a Langmuir cylindrical probe flew aboard the INTERCOSMOS-19, equipped also with an ionospheric sounder besides the other instruments for scientific researches.

Aboard INTERCOSMOS-BULGARIA-1300 satellite, launched on August 7th 1981, there was a payload of 11 instruments, aimed at researching the interactions of ionosphere and magnetosphere. The values measured involve the pa-

parameters of thermal plasma and its drift velocity, the AC and DC electric fields, the magnetic fields of the earth, the energy spectrum of protons and electrons, and the intensity of the atmospheric emissions in the visible and in ultra-violet portion of the spectrum. Recently, on the grounds of these data there has begun the study of the structure of the equatorial ionosphere and of the polar oval, the behaviour of the SAR-arcs, the double electrostatic layers, the particle acceleration, etc.

Bulgarian participation is significant in experimenting rockets of the VERTICAL type, launched from a midlatitude station and reaching an altitude of up to 1500 km. Using the vertical profiles of outer ionosphere provided by the rockets of the VERTICAL-3, 4, 6 and 10, obtained within almost one decade, there were conducted studies on the ion composition, on the structure and dynamics of the ionospheric plasma.

This paper attaches special attention to some investigations, conducted by researchers from the Central Laboratory for Space Research in Sofia. Among the multitude of their findings this paper presents only those which give a complete idea of the physical conditions in outer ionosphere at low and midlatitudes, independently of the fact that these results have been obtained over a period of more than thirteen years.

### Latitude Variations of Ion Density

The latitude variations of ion density have been extensively studied, using data from spherical ion traps (SIT) on board INTERCOSMOS-2 and 8, and those from the retarding potential analyzer (RPA) on OGO-6 satellite\*.

The latitude distribution of  $O^+$  ion density measured by INTERCOSMOS-8 between 280 and 580 km height in the afternoon and evening hours has been analyzed in [1, 2]. Fig. 1 gives profiles of the  $O^+$  density between  $50^\circ$  and  $-50^\circ$  diplatitude for several consecutive longitudes. The local times of the measurements lie between 15.30 and 19.30 h. In the front panel an average satellite altitude shows the dependence of ion density on height. The orbits have been chosen with a view to the satellite passing the equatorial region around the maximum of F-layer where the anomaly is better pronounced. The main feature is a double maximum distribution of ion density. The two crests are situated at about  $15^\circ$  on both sides of the geometrical equator. At longitudes between  $-50^\circ$  and  $7^\circ$  ion density reaches its minimum at about  $10^\circ$  north of the equator. These longitude peculiarities will be analyzed further on. Daytime distribution of ion density around the maximum of the F-layer, shown in Fig. 1, is in full conformity with the results of the previous investigations, for example [3, 4]. Meridional profiles of ion density in the evening hours (17.00-22.30 LT) are shown in Fig. 2. It displays clearly the distortion of the daytime anomaly. The equatorial depletion is now shifted to the north to a latitude of about  $15-20^\circ$ , while the southern crest acquires higher density. A tendency can be observed for the latter crest to shift towards the equator and for the northern crest to disappear. This picture corresponds to a transition stage towards establishing a steady one-maximum distribution during the night [5, 6]. The local minima, appearing in longitude range ( $-50^\circ, 60^\circ$ ), are caused by local dynamics of the F-layer, which will be discussed further in this paper.

Model calculations made in [7, 8] show that the daytime F-layer equatorial anomaly has an upper altitude limit. At altitudes above 700 km the crests

\* Courtesy of WDC-A for R&S

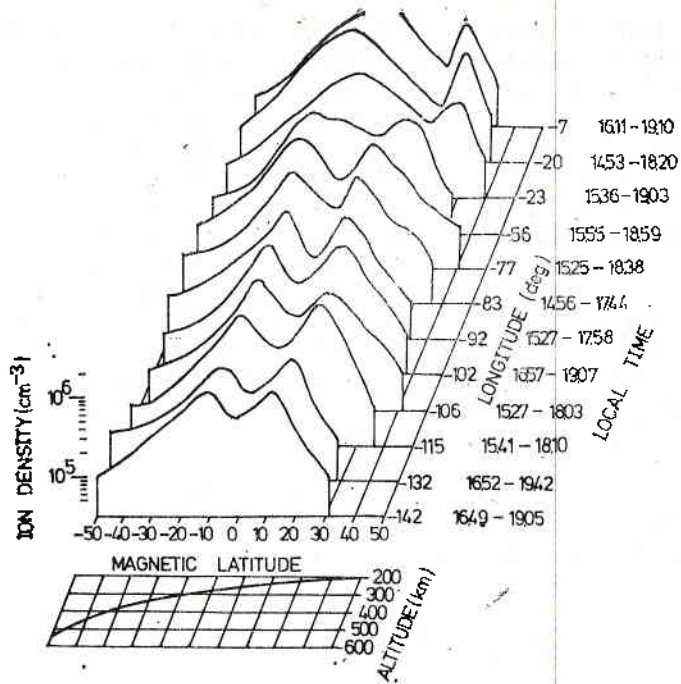


Fig. 1. Daytime  $O^+$  density vs. magnetic latitude. The average altitude of the measurements is drawn in the front panel. Longitudes and local time for every individual profile are given on the right side. The density scale is given on the left side.

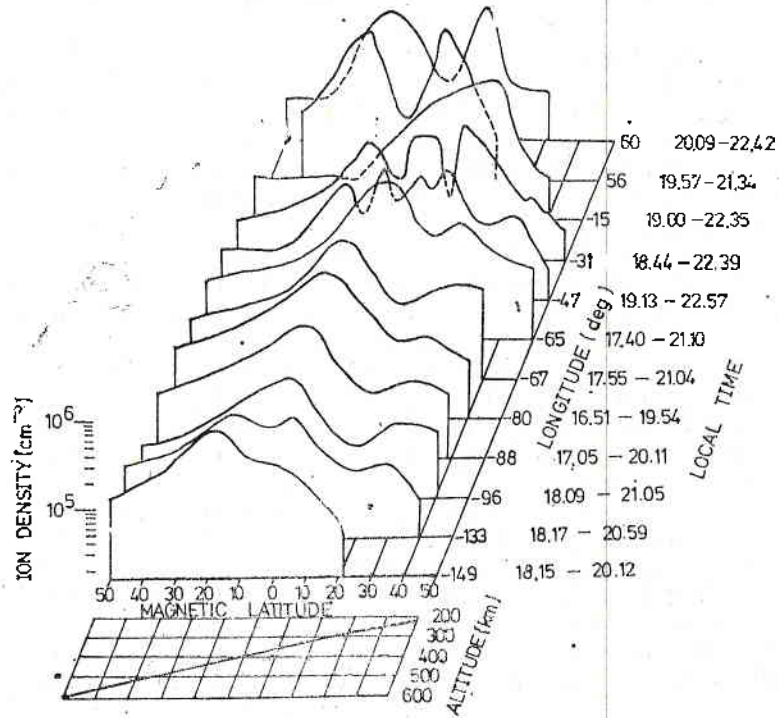


Fig. 2. The same as in Fig. 1. for evening and nighttime conditions.

seem to shift towards each other and at altitudes high enough one-maximum distribution of  $O^+$  ion density is established at the equator. Due to an upward  $E \times B$  drift in equatorial plane the F-layer goes up to 500-700 km. Being lifted

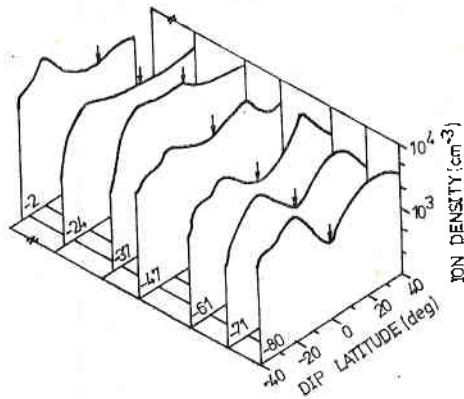


Fig. 3. Nighttime  $H^+$  density over the equator and midlatitudes taken by the INTERCOSMOS-2, January 3-10, 1970

The density scale is shown on the right side. The average satellite altitude is given in the front

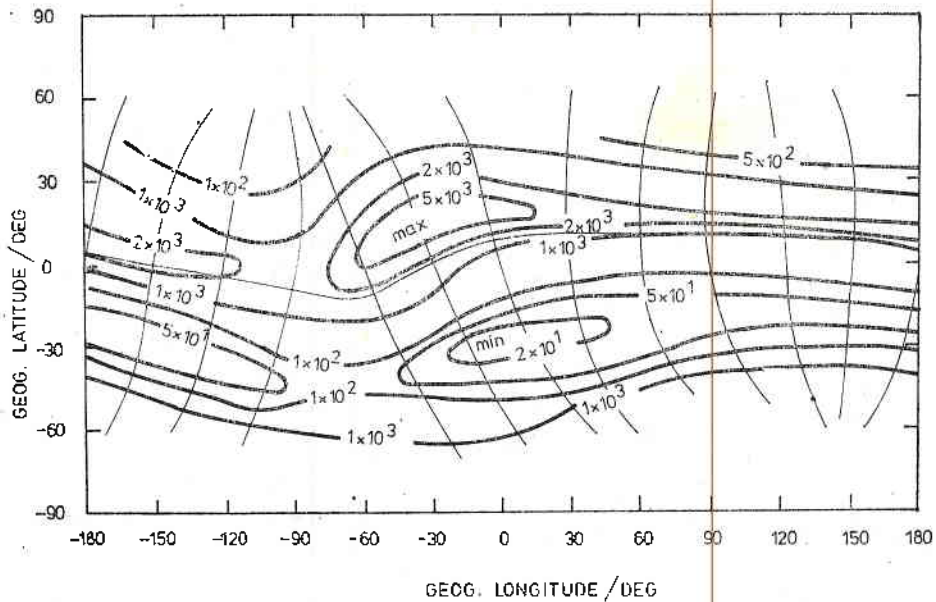


Fig. 4. Contours of constant nighttime  $O^+$  density values for altitudes about 1000 km (the heavy lines)

The data are taken by OGO-6 in the summer of 1969 and 1970. The thin lines represent the magnetic equator and magnetic meridians

higher than the normal midlatitude F-layer, the equatorial F-layer provides the crest regions with ionization which diffuses down along magnetic field lines. Applying this 'fountain effect' to helium and hydrogen ions, the author

in [8] has obtained their latitude distribution. According to this model the helium and hydrogen ion layers which lie above that of the  $O^+$  ions, are lifted by  $E \times B$  drift to greater heights and subsequently they fill magnetic tubes at higher invariant latitudes. An ion distribution measured by a satellite flying at about 1000 km can be represented as follows:

-- Maximal  $O^+$  density and minimal  $H^+$  density at the equator and minimum  $O^+$  and maximum  $H^+$  densities at midlatitudes;

-- The behaviour of  $He^+$  density should be somewhat in the middle: its maximum density should be found equatorward from  $H^+$  maximal density;

-- Minimum  $He^+$  density will appear at the equator, if the  $He^+$  layer is elevated above 1000 km, otherwise a maximum  $He^+$  should be expected there.

Similar behaviour is observed by INTERCOSMOS-2 satellite [9, 10] and ISIS-2 [11]. Latitude distribution of nighttime  $H^+$  density at about 1000-1100 km altitude is shown in Fig. 3 pertaining to a number of INTERCOSMOS-2 transequatorial passes during the period of January 1-14, 1970 [12, 13]. The apogee is near to the equator at a height of about 1100 km. The latitude profiles shown here reveal a two-maximum distribution, resembling the shape of the daytime F-layer equatorial anomaly. The crests of  $H^+$  density are found between  $10^\circ$  and  $30^\circ$  on both sides of the equator. Approximately half a year ago, also in the maximum solar activity period, data of latitude distribution of  $O^+$  density, at about the same heights were collected by OGO-6 satellite [15]. Contours of oxygen ion density obtained by RPA of OGO-6 [14] during the night at 1000-1100 km are plotted on Fig. 4. If we consider now only the latitude variations we see that the oxygen ions have maximal density slightly northwards from the geometrical equator towards the summer hemisphere. At the opposite side of the

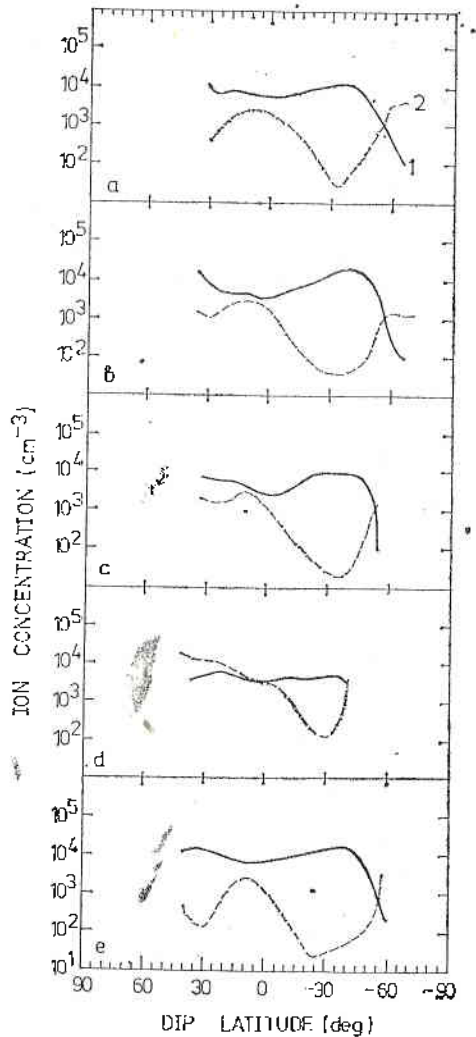


Fig. 5. Nighttime  $O^+$  and  $H^+$  density for five individual passes of OGO-6 in different longitude zones

Apogee of 1090 km is at the dipequator, with the altitude at  $\pm 60^\circ$  dip latitude being about 800 km  
 1 -  $H^+$ ; 2 -  $O^+$ ; longitude: a -  $172^\circ$ , b -  $116^\circ$ , c -  $72^\circ$ , d -  $-40^\circ$ , e -  $-134^\circ$

equator a deep minimum occurs and at some locations the density appears to be as low as 20 ions per cc. A good idea how the latitude distribution of  $H^+$  and  $O^+$  density should look is given by Fig. 5, where RPA data for several passes of OGO-6 over the equatorial region are presented. The shape

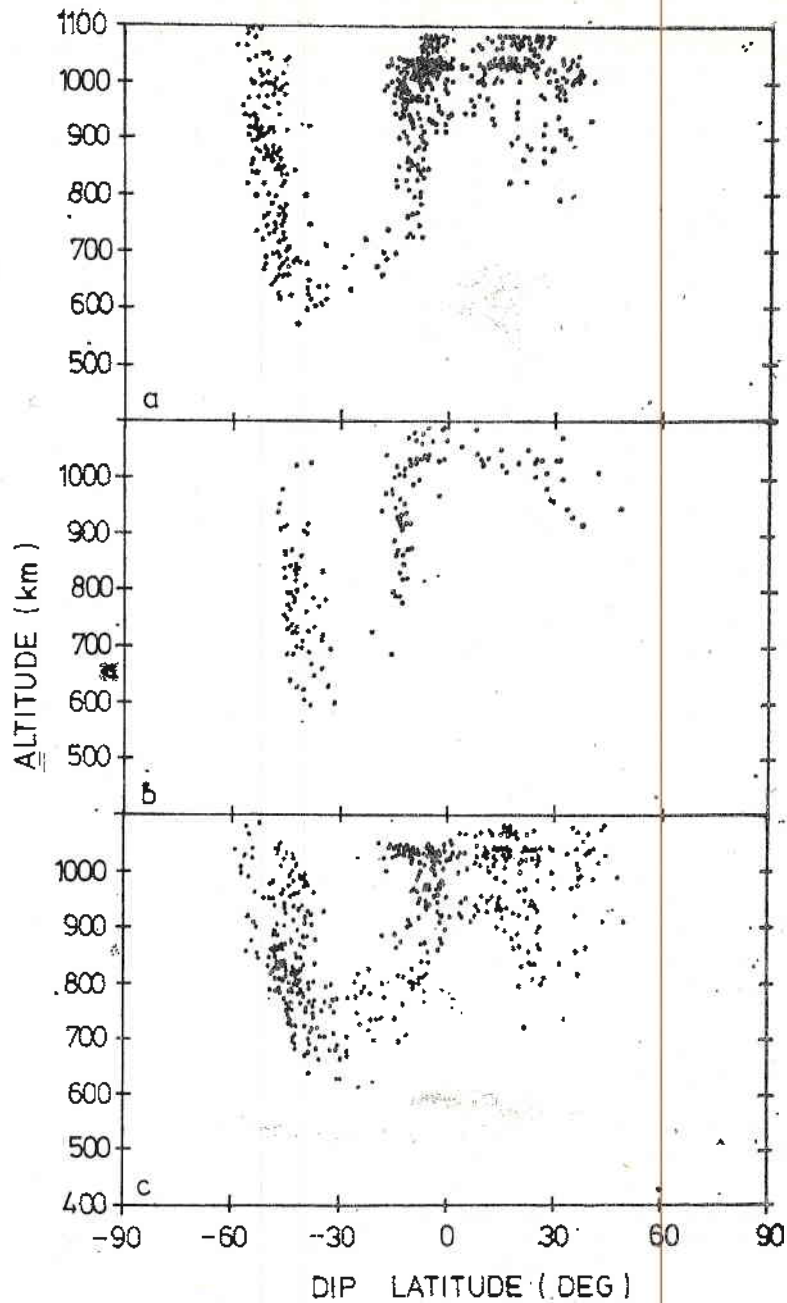


Fig. 6. The altitude dependence of the transition level on the dip latitude in three longitude zones

HMIN=400 and HMAX=1100 indicate the altitude limits over which the data have been taken in summer, nighttime

of  $H^+$  and  $O^+$  densities distribution is in full accord with the 'fountain effect' theory. Winter minimum of oxygen ions at about  $30^\circ$  dip latitude corresponds to a highly exhausted nighttime midlatitude F-region. The relatively shallow summer minimum is a result of the more intensive photoionization during

the day, as well as of the influence of the neutral winds. The action of the latter will be considered further on in the paper. Fig. 5 shows  $H^+$  density almost uniformly distributed over the latitudes considered. Along the orbits where these data have been collected the  $H^+$  and  $O^+$  density reach equal values, several times. The altitude where these densities reach equal values, i. e. the so-called transition level, is a parameter which is used in [15] to visualize some dynamic properties of outer low and midlatitude ionosphere. In Fig. 6 every single point represent a transition level value extracted along the satellite orbit. The transition level (TL) points taken from nighttime data are plotted against their diplatitudes. The three panels of the Fig. 6 show the latitude shape of TL in three longitude intervals: *a* -- Eurasian ( $10^\circ$ ,  $150^\circ$ ); *b* -- Atlantic ( $-60^\circ$ ,  $10^\circ$ ); and *c* -- Pacific ( $150^\circ$ , through  $180^\circ$  to  $-60^\circ$ ). The main feature of these TL profiles is a deep minimum located between  $0^\circ$  and  $40^\circ$  diplatitude, where TL descends to 600 km; while around the equator and poleward end of the latitude region TL is at 1000-1100 km. In [15] it is pointed out that around 18 local time TL is at about 1000-1100 km throughout the region. During the night TL in the equatorial zone remains at the same height, while at midlatitudes a significant decrease of TL occurs. Higher TL values at the poleward edge of the region considered here is due to the abrupt decrease of the  $H^+$  density as it can be seen from the individual passes in Fig. 5. The midlatitude decrease of TL represents the normal nighttime collapse of the F-layer. An interesting feature is the maintenance of the high equatorial TL values during the night. This behaviour is closely associated with  $O^+$  density distribution, shown in Fig. 4. Maximum oxygen ion density occurs at  $59-10^\circ$  latitude in the summer hemisphere. The existing assymetry in  $O^+$  density along the magnetic field lines over the equator gives support to a diffusion flow from summer to winter side. This  $O^+$  flow keeps a higher  $O^+$  density along the magnetic flux tubes close to the equator, because of which TL heights remain high. The latitude at which the height of TL changes abruptly corresponds to those magnetic tubes which limit from above the transequatorial flow of the oxygen ions. Beyond this latitude the direct support of ionization to winter nighttime F-region is strongly restricted, because of the necessity of conversion of oxygen ions into hydrogen ions and vice versa via a charge exchange reaction.

### Longitude Variations

As it has been shown in the preceding section, the latitude profiles of oxygen and hydrogen ions reveal a strong longitude dependence. The overall  $O^+$  density distribution shown in Fig. 4 gives information on large-scale longitude variations of the ion density at a height of 1000 km. The strongest assymetry along the magnetic meridians occurs between  $-40^\circ$  and  $20^\circ$  longitude and the weakest one occurs in neighbouring regions between  $-100^\circ$  and  $-60^\circ$  longitude. The longitude variations of  $O^+$  density at the heights of the maximum F-layer are shown in Fig. 7 [16]. Here the dots represent measured  $O^+$  density at  $30^\circ$  and  $-30^\circ$  diplatitude. The heavy line shows variations of magnetic declination properly adjusted to reveal an excellent correlation with the ion density values. From the *b* section of the figure, representing the summer hemisphere, there can be concluded that the higher ion density along  $30^\circ$  diplatitude is connected with the negative values of the magnetic declination, e. g. the magnetic flux tubes have a westward component. The highest values of the ion density on the summer side of the equator are found at about  $-30^\circ$  diplatitude. The same longitude

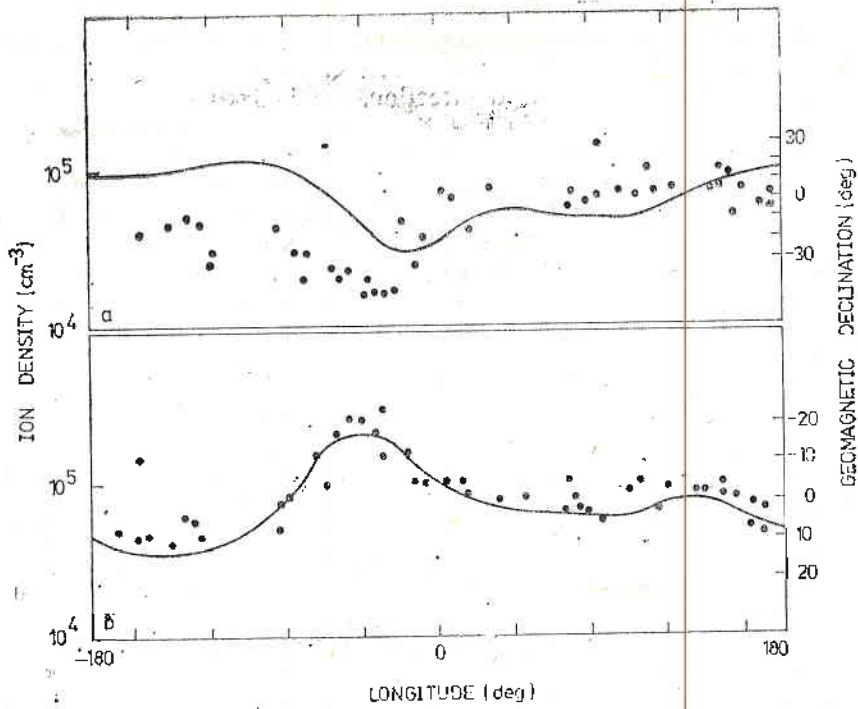


Fig. 7. Nighttime  $O^+$  density vs. longitude taken by OGO-6 at two fixed diplattitudes

The magnetic declination has a scale on the right. This line does not represent an average curve over points, but was adjusted to match the  $O^+$  density variation. *a* - altitude 650-900 km, diplatitude  $-30^\circ$ , local time (LT) 22.00-22.30 h; *b* - altitude 450-500 km, diplatitude  $30^\circ$ , LT 22.30-23.00 h

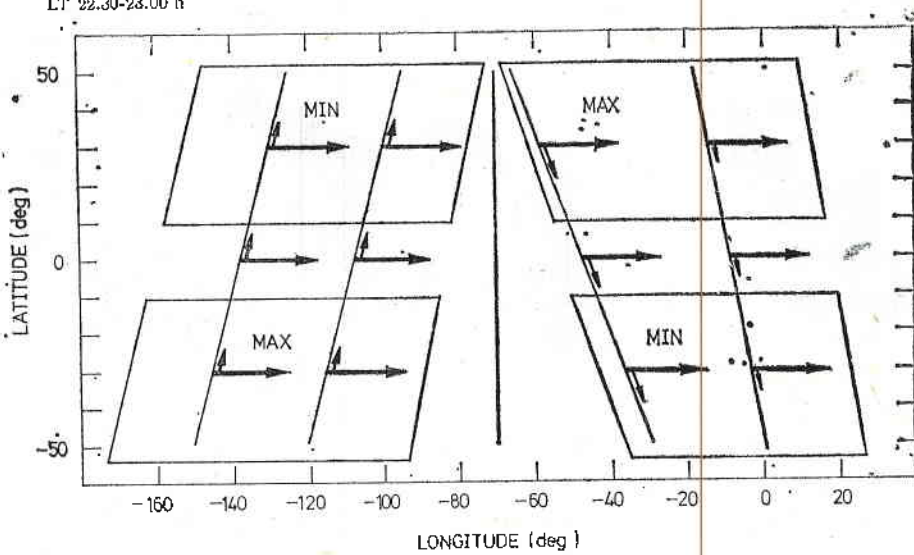


Fig. 8. A sketch representing the neutral wind action on ionization

region from the winter side shows the lowest densities. This behaviour corresponds well to that shown in Fig. 4. A reasonable explanation, given in [17], is demonstrated in Fig. 8. The winds flowing at F-layer heights, preferably



n west-east direction, experience a drag force upon ionization, if the magnetic meridians differ from the north-south direction. Depending on the component of magnetic field lines in the wind direction, the ionization is dragged upward or downward. The light lines in Fig. 8 represent the magnetic field lines in a geographic frame of coordinates. The heavy arrows show the neutral wind direction, and the smaller arrows give the magnitude and the direction of the ion drag along the magnetic field lines. The regions where a satellite could measure enhanced or depleted ionization are also indicated in the figure. The zones marked by MAX correspond to an elevation of the F-layer upwards, and those marked by MIN correspond to a pushing of the F-layer downwards. The sketch in Fig. 7 is in agreement with these in Fig. 4 and 5.

### Irregularity Structure

The magnetic field configuration defines not only ionospheric plasma dynamics, but the appearance of irregularity structure as well. With the help of INTERCOSMOS-2 in [18, 19] the character and size of the irregularities in the equatorial F-region in the period of low solar activity have been studied. In Fig. 9 the latitude profiles of the  $O^+$  density between 280 km and 580 km are displayed. In two cases of the profiles the occurrence of irregularities is indicated by small bars. This shows that irregularities are found mainly between  $-50^\circ$  and  $-10^\circ$  longitude and are strongly coupled with sharp depletions in ion density. Similar individual passes of the same satellite are shown in Fig. 10 [20].

The minima in the density depletions are defined by the threshold sensitivity of the ion traps but other measurements, for instance [21], show that such a decrease reaches three orders of magnitude.

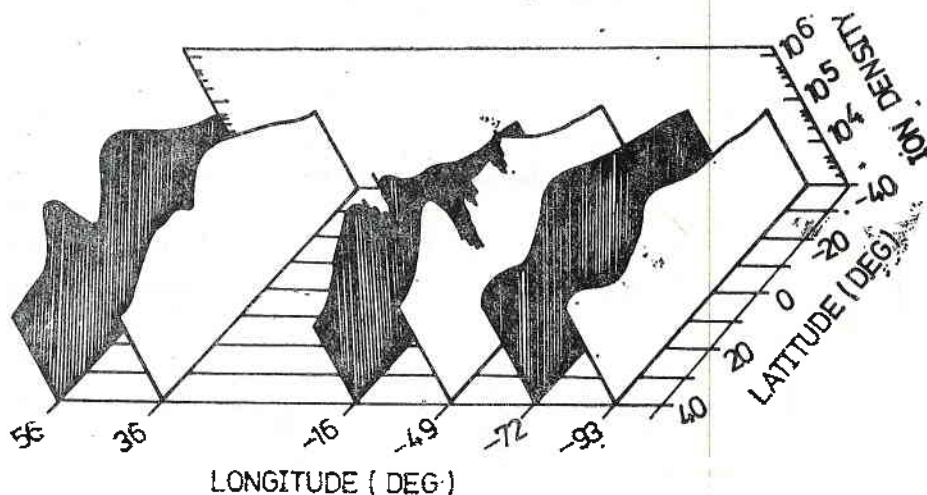


Fig. 9.  $O^+$  density profiles at different longitudes in D months

Vertical bars in the profiles at  $-16^\circ$  and  $-49^\circ$  longitudes indicate the presence of irregularity structure; LT 19.40-22.30 h

Irregularity structure at heights of about 1000 km has been observed by the INTERCOSMOS-2 satellite. In Fig. 11 parts of satellites trajectories with irregularities of over 7% of ion current are indicated. The heavy line represents the geomagnetic equator in a geographic frame of coordinates. The space

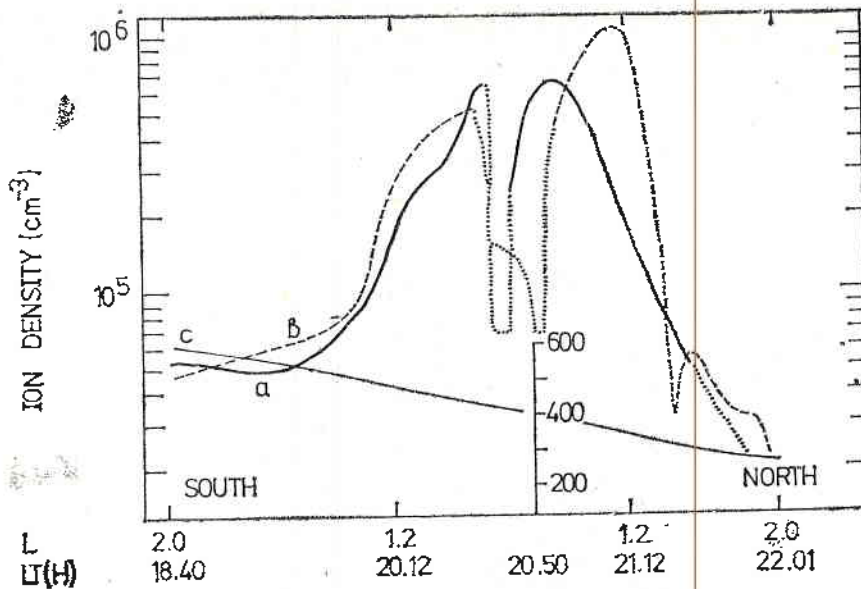


Fig. 10.  $O^+$  density obtained in two consecutive orbits of INTERCOSMOS-8. The portions of the curves around the equator drawn by dots show the presence of small-scale irregularity structure. The bottoms of ion depletions in the equatorial region represent the sensitivity threshold of the instrument: *a* - longitude  $39^\circ$ ; *b* - longitude  $13^\circ$ ; *c* - the average altitude.

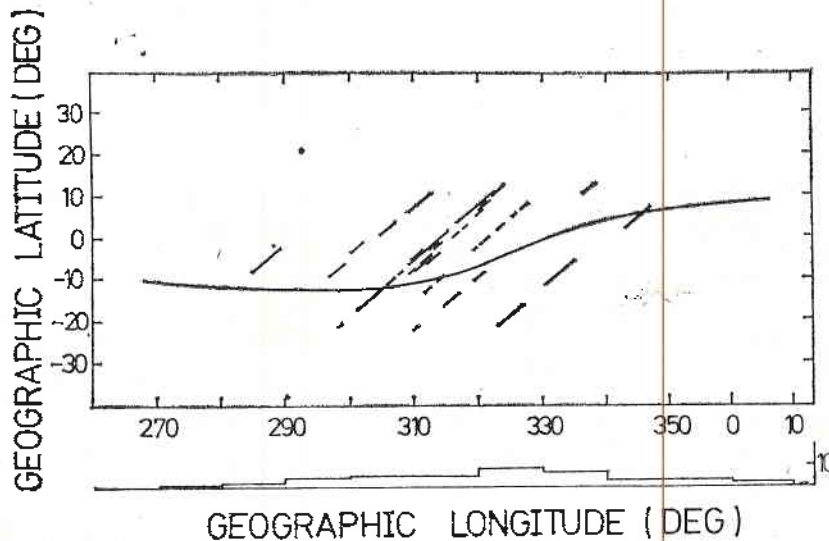


Fig. 11. Geographic distribution of irregularity structure at altitudes of about 1000 km measured by INTERCOSMOS-2 in the winter of 1969, where the dominant ion was  $H^+$ . LT 20.00-06.00 h.

resolution of the measurements is sufficient to detect irregularities, as low as 2 km in size. The histogram at the bottom of the figure shows the number of transits in each  $10^\circ$  longitude interval used to construct the figure. It is obvious that the probability for the occurrence of irregularities is longitude-

dependable. In the region considered the irregularity structure appears between  $-80^\circ$  and  $-20^\circ$  longitude. As it has been shown above, in this region the transequatorial plasma flow induced by neutral winds is most intensive. It is clear that the irregularity generation is somehow influenced by the interaction

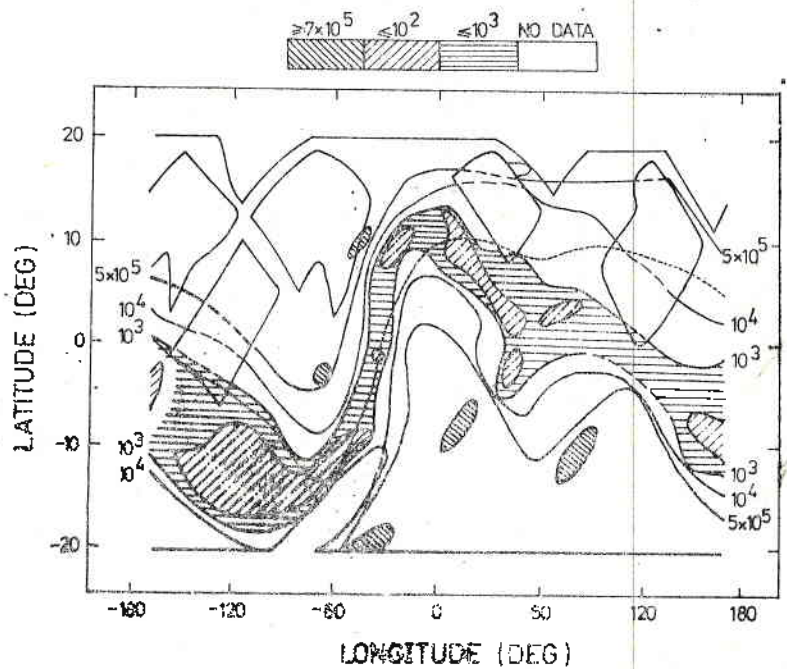


Fig. 12. Contours of  $O^+$  density measured by BIMS on AE-E satellite in the winter of 1977-1978

between neutral winds at the F-region heights and the ionosphere. In [18] large scale plasma irregularities are considered as a result of a direct action of meridional winds over the ionosphere.

Fig. 12 shows the contours of  $O^+$  density measured at 270-320 km between 18 and 24 h local time by Bennet ion mass spectrometer (BIMS) on AE-E in winter 1977-1978. The shaded area marks the regions where  $O^+$  number density below  $10^3 \text{ cm}^{-3}$  have been recorded. These depletions are placed mainly on the summer side of the equator, being closer to it in the regions with higher magnetic declination. Theoretical contours of the vertical ion drift are shown in Fig. 13. For these calculations simple models of electric field and winds are considered varying only in latitude. Diffusion velocity is calculated for a neutral density of  $5 \times 10^6 \text{ cm}^{-3}$  at the maximum of F-layer. The comparison of Fig. 12 and Fig. 13 shows an excellent coincidence between the ion drift maximum and the  $O^+$  density minima in the whole of the longitude interval.

Many researchers associate the occurrence of irregularities in the F-layer with the generation of the so-called 'bubbles' [22, 23]. The bubbles being areas of depleted ion density are generated at the bottom of the F-layer where large gradients of ion density exist [24]. Once generated, the bubbles move upwards almost perpendicularly to the magnetic field lines and can reach heights of 1000 km. Born in a certain magnetic flux tube in the equatorial plane, the

depleted area creates diffusive flows whose magnitude depends on the velocity of the bubbles moving upwards. As a result of this, the total ionization in this particular flux tube can decrease significantly. According to [25], the bubbles create both vertically elongated depletions and depletions along the magnetic

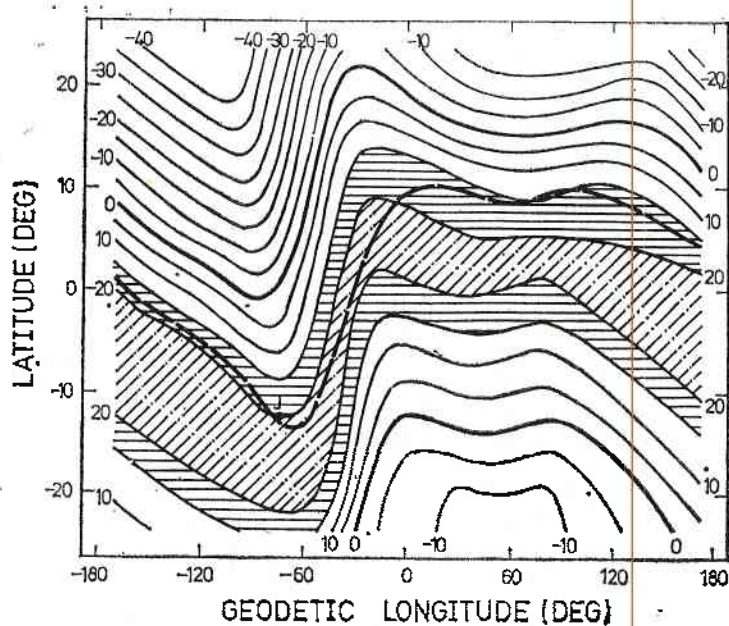


Fig. 13. Contours of vertical ion drift velocity (m/s) calculated under possible winds and electric field conditions in D months  
Positive velocity is upwards; altitude 300 km; LT 19.00-22.00 h

field lines. Taking into consideration such a complicated structure of ion density distribution, there can be drawn a parallel between Fig. 11 and Fig. 12. There is an impression that they are not so much consistent, although they represent one and the same season in the solar maximum years. A possible explanation might be that the two figures represent different types of irregularities. The INTERCOSMOS-2 data represent small-scale irregularities: 2-5 km in size, while AE-E data reveal large-scale plasma depletions which may not be accompanied by small-scale irregularities. Now it is considered [25] that the bubbles generation is due to, or is accompanied by, strong plasma turbulence which dissipates as bubbles move upwards. At higher altitudes the smaller-scale irregularities get smoothed out due to the large diffusion coefficient. The smaller-scale irregularities appear in Fig. 11 at the region of maximal transequatorial plasma transport. Apart from the highest magnetic declination, the plasma flow over the equator is favoured by the lowest value of L parameter. The latter implies that magnetic force line emerging from the Earth at one and the same geomagnetic latitude will pass over the equator in a region considered by 150 km lower than over the other longitudes. The net plasma flow driven through by neutral winds is most intense in this valley and can elevate irregularities to heights observed in Fig. 11.

*Acknowledgement:* The author is obliged to Prof. K. Serafimov, Ts. Dachev, L. Bankov and other collaborators from the Central Laboratory for Space Research whose works have been used in this paper.

## References

1. Serafimov, K., I. Kutiev, J. Arsov, Ts. Dachev, G. Stanev, G. Gdalevich, V. Afonin, V. Gubsky, V. Ozerov, Ya. Schmilauer. — *Space Res.*, 16, 1976, 27.
2. Serafimov, K., I. Kutiev, J. Arsov, Ts. Dachev, G. Stanev, G. Gdalevich, V. Afonin, V. Gubsky, V. Ozerov, Ya. Schmilauer. — *Space Res. in Bulgaria*, 1, 1978, 5.
3. Eccles, D., J. W. King. — *Proc. IEEE*, 57, 1969, 1112.
4. Goldberg, R. A. — *Proc. IEEE*, 57, 1969, 1119.
5. Anderson, D. N. — *Planet. Space Sci.*, 21, 1973, 409.
6. Goldberg, R. A., P. C. Kendall, E. R. Schmerling. — *J. Geophys. Res.*, 69, 1964, 417.
7. Rush, C. M., S. U. Rush, L. R. Lyons, S. V. Venkataswaran. — *Radio Sci.*, 4, 1969, 829.
8. Chandra, S. — *J. Atm. Terr. Phys.*, 37, 1975, 359.
9. Gdalevich, G. L., B. N. Gorojankin, Ts. Dachev, I. Kutiev, K. Serafimov. — *Compt. rend. Acad. Bulg. Sci.*, 26, 1973, 755.
10. Gdalevich, G. L., B. N. Gorojankin, I. Kutiev, D. Samardjiev, K. Serafimov. — *Kosmicheskie Issledovaniya*, 11, 1973, 2 (Russ.).
11. Hoffman, J. H., W. H. Dodson, C. R. Lippincott, D. H. Hammack. — *J. Geophys. Res.*, 79, 1974, 4246.
12. Gdalevich, G., B. Gorojankin, Ts. Dachev, I. Kutiev, K. Serafimov. — *Bull. Inst. of Geophys.*, 20, 1974, 39 (in Russian).
13. Gdalevich, G., B. Gorojankin, I. Kutiev, D. Samardjiev, K. Serafimov. — *Bull. Inst. of Geophys.*, 19, 1974, 71 (Russ.).
14. Hanson, W. B., S. Sanatani, D. Zuccaro, T. Flowerday. — *J. Geophys. Res.*, 75, 1970, 5483.
15. Kutiev, I., R. Heelis, S. Sanatani. — *J. Geophys. Res.*, 85, 1980, 2366.
16. Serafimov, K., Ts. Dachev, L. Bankov, I. Kutiev. — Reprint GLSR 8301, 1983.
17. Dachev, Ts., G. C. G. Walker. — *J. Geophys. Res.*, 87, 1982, 7625.
18. Dachev, Ts. Private communication, 1981.
19. Bankov, L., Ts. Dachev. — *COSPAR Space Res.*, 1978, 273.
20. Serafimov, K., Ts. Dachev, I. Kutiev, G. Gdalevich. — *Proc. of the Symp. on Magnetospheric Ionospheric Physics. Sun and Solar Wind. Gorbunovo, 1979*, 374 (in Russian).
21. Hanson, W. B., S. Sanatani. — *J. Geophys. Res.*, 78, 1973, 1167.
22. Dyson, P., R. Benson. — *Geophys. Res., Lett.*, 5, 1978, 795.
23. Ossakov, S., P. Chaturvedi. — *J. Geophys. Res.*, 83, 1978, 2085.
24. Chaturvedi, P. K. — *J. Geophys. Res.*, 83, 1978, 4219.
25. Tsunoda, R., R. Livingstone, J. P. McClure, W. B. Hanson. — *J. Geophys. Res.*, 87, 1982, 9171.

## Внешняя атмосфера на средних и низких широтах

*И. С. Кутиев*

(Резюме)

Автор делает попытку обобщить некоторые результаты спутниковых исследований средней и нижней ионосферы, проведенных в Центральной лаборатории космических исследований в Софии за последние 13 лет. Приведены данные о широтной и долготной структуре этой области в свете современных пониманий происходящих в ней процессов и явлений. Отдельно рассматривается поведение околорезонансной части слоя и области на высоте около 1000 км. Эти две области находятся в контакте и взаимодействии посредством процессов диффузии и обмена зарядами. Рассмотрены долготные особенности в распределении ионной плотности как результат взаимодействия нейтральных ветров при разных конфигурациях магнитного поля. Уделено внимание появлению неоднородностей в экваториальном районе и причине образования неоднородной структуры.